2.N

Nuclear Physics A280 (1977) 267—284; © *North-Holland Publishing Co., Amsterdam*

ON THE INTERPRETATION OF EVAPORATION RESIDUE MASS DISTRIBUTIONS IN HEAVY-ION INDUCED FUSION REACTIONS

F. PÜHLHOFER†

Gesellschaft für Schwerionenforschung, Darmstadt, Germany

Received 27 September 1976
(Revised 11 November 1976)

Abstract: Evaporation residue mass distributions measured recently for several heavy-ion induced fusion reactions are analyzed. The reactions investigated are ^{19}F on ^{12}C (E_{lab} = 50, 63 and 76 MeV), ^{19}F on ^{27}Al (E_{lab} = 40, 63, 76 and 92 MeV) and ^{16}O on ^{27}Al (E_{lab} = 30, 40, 60 and 80 MeV). Starting from the assumption that a compound nucleus is formed which decays by multiple emission of neutrons, protons, α-particles and γ-rays with probabilities as predicted by the statistical theory the mass spectra of the stable or long-lived products are calculated. It is shown that they are in good agreement with the experimental data, if reasonable assumptions are made about the level densities and the shape of the yrast line. The possibility to use these methods for studying the properties of highly excited nuclei at high angular momentum is investigated.

1. Introduction

Recent advances in time-of-flight techniques have made it possible to investigate heavy-ion induced compound-nucleus reactions experimentally by detecting the evaporation residues at small angles relative to the beam direction and measuring their mass distribution. A large recoil energy and consequently a heavy projectile are required for good identification of the reaction products in a detector telescope. On the other hand, for not too massive compound nuclei the transverse momentum due to the evaporation of particles results in sufficient deflection of the residual nuclei out of the beam direction. Examples of such experiments, in which the fusion products were resolved by mass, may be found in refs. [1-6]). Compared to similar studies using in-beam γ-ray spectroscopy the time-of-flight method has the advantage of having a detection efficiency which is independent of the nature of the product nucleus, but it is limited to light to medium-weight systems ($A_{CN} \leqq 100$) and high recoil energies.

A typical experimental result is shown in fig. 1. In this example, the compound nucleus ^{46}Ti is formed at 70 MeV excitation energy in a fusion reaction between ^{19}F and ^{27}Al. The peaks in the mass spectrum of the evaporation residues indicate its dominant decay modes, which, in this case, are the emission of four nucleons, one α-particle together with three nucleons and two α-particles together with two nucleons. These assignments are based on the energy balance of the reaction, the shape of

† On leave from Fachbereich Physik, Universität Marburg, Germany.

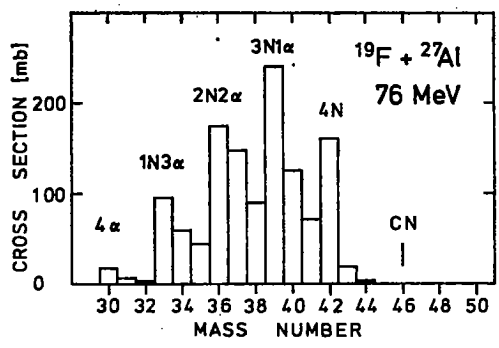

Fig. 1. Mass distribution of the evaporation residues in the fusion reaction of 76 MeV ^{19}F on ^{27}Al. Data from Pfeffer *et al.* [6]).

the spectra and angular distributions of the product nuclei and finally the comparison with deexcitation calculations. It is obvious that the mass distribution of the evaporation residues provides a quantitative survey of the intensities of all particle- decay channels of the compound nucleus. Whereas the position of the maxima is to a large extent governed by kinematics, their relative intensities can not be understood by trivial arguments. It seems logical to use this information for studying nuclei at high excitation and high angular momentum.

The subject of this work is a theoretical analysis of such data obtained for heavy-ion induced fusion reactions. The assumption is made that projectile and target form a compound nucleus in statistical equilibrium, and the Hauser-Feshbach formula together with the statistical nuclear model are applied in order to calculate the intensities of the various decay chains. The model and in particular the parametrization used here for the level densities are described in the next section. The theory is then applied to data obtained recently [2, 6–8]) for fusion reactions between $^{19}F+^{12}C$, $^{16}O+^{27}Al$ and $^{19}F+^{27}Al$ and the parameters of the calculations are discussed. The essential questions to be investigated are whether the mass distributions of the evaporation residues can be understood quantitatively, and which information on nuclear properties are contained in them.

2. Theory

2.1. INTRODUCTORY REMARKS

In this section we quote assumptions and formulae on which our calculations concerning the interpretation of the evaporation residue mass distributions are based. As mentioned, we start from the assumption that a compound nucleus is formed in statistical equilibrium with respect to all degrees of freedom. Its spin distribution is usually derived from the known fusion cross section using a strong-absorption model. The decay of the compound nucleus by particle emission is then calculated from the Hauser-Feshbach formula. The decay probabilities are determined by the statistical

weight of the final states and the barrier penetrabilities for the various channels. Generally, only neutron, proton, α-particle and γ-ray emission have to be taken into consideration. The influence of deuteron emission was investigated and found to be negligible for the reactions studied. In spite of its strong increase with angular momentum [9]), evaporation of complex particles like ^{6}Li is also expected to be, on the whole, an unimportant decay channel. Level densities for the product nuclei are calculated from a formula which is derived from the Fermi gas model. In the region of low excitation energies the parameters can be determined empirically. However, special attention is required for the region of high excitation and, because of the high angular momenta involved in heavy-ion reactions, for the spin-dependence of the level densities. This will be discussed in detail. Finally, a computer code is described, which calculates the deexcitation of the compound nucleus by multiple particle and γ-ray emission and determines the cross section for long-lived or stable product nuclei in the ground state, i.e. those which are detected in the experiment. The calculations reported here are in principle similar to those of Grover and Gilat [10]), Blann [11]), Ruddy *et al.* [12]) and Uhl [13]). We refer in particular to the extensive discussion in ref. [10]).

In principle, the calculated cross sections can only be compared to data which are averaged over energy and, hence, over statistical fluctuations. In most of the experiments discussed here, the averaging due to a finite target thickness is already sufficient. Moreover, the measured evaporation residue cross sections are integrated over the energies of all intermediate nuclei in the decay chain, often also over different decay chains leading to the same product (like αpn, pαn and so on). Therefore, it is not expected that statistical fluctuations have to be considered. However, distinct resonances like the one observed [14]) in the channel ^{16}O+^{12}C are not necessarily averaged out.

Fission as a possible deexcitation mode has been neglected. This seems justified, since in the nuclei considered here it will be important, if at all, only at the highest angular momenta, consequently only in the first decay step. In this case, it can be taken into account by a proper choice of the angular momentum range in the compound nucleus, i.e. by cutting off the highest partial waves. Also neglected is the possibility that decays may occur before statistical equilibrium is reached. The influence of this pre-equilibrium emission is hard to estimate. It probably leads to a slight preference for nucleon evaporation and to higher kinetic energies in the first decay step. The omission can be justified by the success of the theory. It is plausible, since in a heavy-ion collision the energy is, from the very start, shared by a large number of nucleons.

2.2. COMPOUND-NUCLEUS FORMATION

The partial cross section for formation of a compound nucleus of spin J and parity π from a projectile and a target nucleus (spins J_P, J_T) at a c.m. energy E is given by [15, 16])

$$\sigma(J,\pi) = \pi\lambda^2 \frac{2J+1}{(2J_P+1)(2J_T+1)} \sum_{S=|J_P-J_T|}^{J_P+J_T} \sum_{\substack{L=|J-S| \\ [\pi]}}^{J+S} T_L(E). \qquad (1)$$

The transmission coefficients T_L are assumed to depend only on the energy and the orbital angular momentum L. Here $S = J_P + J_T$ is the channel spin. The summation over L is restricted by the parity selection rule $\pi = \pi_P \pi_T (-1)^L$.

For the strongly absorbed heavy ions, the transmission coefficients T_L have a very simple behavior as function of angular momentum. In the calculation they are approximated by a Fermi distribution

$$T_L = \frac{1}{1+\exp\left[-(L-L_0)/d\right]}, \tag{2}$$

with the parameters L_0 and d. Here L_0 is chosen so that the measured fusion cross section

$$\sigma_{CN} = \sum_{J,\pi} \sigma(J,\pi) \tag{3}$$

is reproduced. In this way, one corrects for the presence of direct reactions, which are usually assumed to be surface reactions. Little is known about the diffuseness d. We chose values similar to those obtained from optical-model calculations.

2.3. DECAY PROBABILITIES

The expression for the particle emission probability is derived from the inverse cross sections written in terms of transmission coefficients using the reciprocity theorem [15,-17]). We follow the presentation of Thomas [16]). The rate $R_x d\varepsilon_x$ for emitting a particle x from an excited nucleus 1 (excitation energy E_1, spin J_1, parity π_1) to form a product nucleus 2 (at E_2, J_2, π_2) is

$$R_x d\varepsilon_x = \frac{1}{\hbar}\Gamma_x(\varepsilon_x) = \frac{\rho_2(E_2, J_2, \pi_2)}{2\pi\hbar\rho_1(E_1, J_1, \pi_1)} \sum_{S=|J_2-s_x|}^{J_2+s_x} \sum_{\substack{L=|J_1-S| \\ [\pi]}} T_L^{\alpha}(\varepsilon_x) d\varepsilon_x, \tag{4}$$

where ε_x is the kinetic energy of particle x, equal to $E_1 - E_2 -$ separation energy; s_x is the spin of particle x, L is its orbital angular momentum, and $S = J_2 + s_x$ is the channel spin.

The transmission coefficients T_L^{α} for the scattering of particle x on nucleus 2 are obtained from the optical model using average parameters. Spin-orbit effects are again neglected. In the summation over L, parity conservation has to be taken into account. The level densities ρ will be discussed in the following subsection.

Following Grover and Gilat [10]) and Ruddy *et al.* [12]) we use a formula similar to the previous one for the γ-decay:

$$R_\gamma d\varepsilon_\gamma = \frac{1}{\hbar}\Gamma_\gamma(\varepsilon_\gamma) = \frac{\rho_1(E_2, J_2, \pi_2)}{2\pi\hbar\rho_1(E_1, J_1, \pi_1)} \sum_L \xi_L f_L(\varepsilon_\gamma) d\varepsilon_\gamma. \tag{5}$$

Here, L denotes the multipolarity of the γ-ray, and $\xi_L f_L(\varepsilon_\gamma)$ are energy dependent strengths. In our calculations, only E1, M1 and E2 transitions are considered. The energy dependence is assumed to be $f_L(\varepsilon_\gamma) = \varepsilon_\gamma^{2L+1}$, which is the basic energy dependence for single-particle transitions. Above 22 MeV, the approximate location

of the giant dipole resonance in the mass region considered in this paper, $f_L(\varepsilon_\gamma)$ is assumed to drop to zero at the arbitrarily chosen energy of 32 MeV. In view of the insensitivity of the results to these details this rough model seems to be sufficient. The constants ξ_L can be estimated from the strengths of transitions between low-lying states in the mass region of interest or from the Weisskopf single-particle estimate.

In the calculations described below not the absolute decay rates, but only branching ratios for the various particle and γ-decay channels are used. Normalization is obtained from the assumption that other decay modes than the ones included are negligible.

2.4. LEVEL DENSITIES

The level densities comprise a crucial point of the theory. In the heavy-ion induced fusion reactions of interest here the region of high excitation and in particular the levels at high angular momentum have an essential influence on the deexcitation cascade. In principle, the analysis offers the possibility to study, for example, the position of the yrast line. This, however, requires that the level densities are parametrized by means of a reasonable model containing the relevant degrees of freedom.

We start from Lang's formula [18]), which is based on a Fermi gas model with equidistant levels. According to Gilat [19]) the spin dependence obtained from this formula is in reasonable agreement with the results of more realistic level density calculations. The density ρ of levels of spin J at an excitation energy E is given by

$$\rho(E, J) = \omega(E, M = J) - \omega(E, M = J+1), \tag{6}$$

with the state densities

$$\omega(E, M) = \omega(E - M^2/aR, 0), \tag{7}$$

$$\omega(E, 0) = \frac{1}{12\sqrt{R}a^2t^3} \exp(2\sqrt{aU}), \tag{8}$$

and the equation of state

$$U = E - \Delta = at^2 - \tfrac{1}{2}t. \tag{9}$$

Here, a is the usual level density parameter, which determines the energy dependence, Δ is a pairing energy, which determines the zero point of the effective excitation energy $U = E - \Delta$, and t is the thermodynamic temperature given by the equation of state. The spin dependence is determined by the parameter $aR = 2\mathcal{I}/\hbar^2$, where $\mathcal{I}$ can be regarded as an effective moment of inertia. The latter is parametrized by writing $\mathcal{I} = \frac{2}{5}mr^2$ with $r = r_0A^{\frac{1}{3}}$. This defines an effective radius parameter r_0. The level density formula implies an yrast line

$$E_{\text{rot}}(J) = J(J+1)/aR + \Delta = \frac{J(J+1)\hbar^2}{2\mathcal{I}} + \Delta. \tag{10}$$

In view of the very large range of excitation energies to be considered here it seems

unreasonable to use energy-independent parameters. Therefore, we divide the energy scale into three regions:

Region I (low excitation energy, $E < 3$ to 4 MeV): Here, the experimentally known levels are used. In some cases, high-spin states are known from (HI, xnγ) reactions at higher excitation energy. They are included as yrast levels in region II.

Region II (medium excitation energy, $4 < E < 10$ MeV): In this region, the analytic level density formula is applied. The parameters a and Δ can be determined empirically for each nucleus, as has been done, for example, in the work of Vonach *et al.* [20]) and Dilg *et al.* [21]). Uncertain is the value of aR (respectively r_0). It can be determined approximately from the position of high-spin states. For the dependence of ρ on parity a function was chosen, which varies linearly from the empirical value at low excitation energy to an equipartition at an energy to be chosen individually ($\approx$ 10 to 15 MeV).

Region III (high excitation, $E > E_{\mathrm{LDM}}$): Very little is known about the level densities in this region. We assume that at a sufficiently high excitation energy E_{LDM} all nuclei behave as predicted by the liquid-drop model. We use the analytical form of the Fermi gas level density given above. Both parities are assumed to be equally probable. The parameter $a = a_{\mathrm{LDM}}$ is set equal to $\frac{1}{8}A$ MeV^{-1}. This corresponds roughly to the smooth background of a when plotted as a function of mass number A, disregarding shell effects. The parameters Δ_{LDM} are calculated from the assumption, that the virtual ground state for the level density in this region should coincide with the ground-state energy of a spherical liquid drop, which can be calculated from the Myers-Swiatecki mass formula [22]), but without shell and even-odd corrections. The moment of inertia, which determines the spin dependence, is taken to be that of a deformable liquid drop with gyrostatic motion. Average rms radii derived from electron scattering data are used, as cited by Myers [23]). The deformability under rotation is taken into account by assuming $\mathcal{I} = \mathcal{I}_{\mathrm{sphere}}(1+\delta L^2)$. This L-dependence is suggested by a simple model for a rotating liquid drop. It can be regarded as the first term in an expansion of the moment of inertia obtained by Cohen, Plasil and Swiatecki [24]), and we used their results for determining the deformability δ.

The level density parametrization is based on the assumption that above some excitation energy E_{LDM} the influence of the individual shell structure of a nucleus on the parameters a and Δ vanishes, as is suggested by theoretical investigations [25, 26]). It is, however, a simplification to assume energy-independent parameters even at high energies, as shown by Williams, Chan and Huizenga [26]). This is only justified as long as the results remain insensitive. From the calculations of the authors mentioned [26]) it follows that the transition energy E_{LDM} lies in the range between 30 and 40 MeV. However, in the heavy-ion reactions considered in this work, increasing excitation energy is always connected with increasing average angular momentum. Therefore, the effects of both cannot be separated. Through the deformation of the nucleus due to angular momentum, the latter can be more effective in suppressing shell effects than excitation energy. This was one of the reasons why a lower value for

E_{LDM} ($\approx$ 15 to 20 MeV) was chosen. Between regions II and III the parameters are interpolated linearly.

At high angular momentum the shape of a nucleus is expected to deviate considerably from a sphere. This was shown by Cohen, Plasil and Swiatecki [24]) in calculations based on the liquid-drop model.

The deformations are included here by introducing an angular momentum dependent moment of inertia. In this way, one obtains an yrast line deviating from that of a rigid sphere as shown in fig. 2 and a smooth continuation of the level density to the yrast line. This implies an enhancement of $\rho(E, J)$ compared to the undeformed case. Since in heavy-ion reactions at energies above the Coulomb barrier the population of the compound nucleus extends to high spins (see fig. 2), an appreciable fraction of the deexcitation cascade takes place in the vicinity of the yrast line and will therefore be sensitive to its shape and the spin dependence of the level densities in this region. Because of the connection between the shape of the yrast line and the shape of the nucleus itself one may hope to obtain information on the latter by measuring the decay probabilities, in particular the ratio between nucleon and α-particle emission.

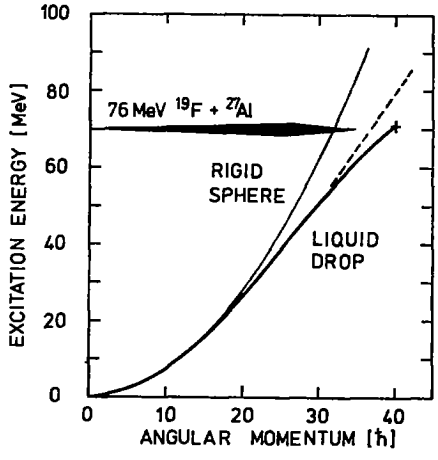

Fig. 2. Rotational energy of a nucleus ($A = 41$, $r_0 = 1.29$ fm) assuming rigid rotation of a sphere and of a deformable liquid drop [24]), respectively. The approximation of the latter using $\mathcal{I} = \mathcal{I}_{\text{sphere}}(1+\delta L^2)$ with $\delta = 2.5\times10^{-4}$ is shown by the dashed line. For comparison, the spin distribution of the compound nucleus in the reaction 76 MeV ^{19}F on ^{27}Al is indicated.

In table 1 the parameters necessary for defining the level densities $\rho(E, J)$ are summarized. It should be emphasized, that there are only a few parameters, which are unknown or badly fixed and critical for the results. Except for r_0, which influences the spin dependence in region II, these are mainly the transition energy E_{LDM} for the beginning of the liquid-drop region and the parameters r_{0LDM} and δ determining the spin dependence and the yrast line at high excitation.

TABLE 1
Level density parameters

Region I	
	Individual levels for each nucleus
Region II	
	Empirical level density parameters a, Δ for each nucleus
	Radius parameter r_0 for effective moment of inertia
	Experimental yrast levels, if available
	Parity distribution
Region III	
	Transition energy E_{LDM}
	Level density parameters a_{LDM} ($\approx \frac{1}{9}A$ MeV^{-1})
	Virtual ground-state energy Δ_{LDM} for each nucleus
	Radius parameter $r_{0\mathrm{LDM}}$
	Deformability δ

2.5. COMPUTER CODE

The calculation of the decay of a highly excited compound nucleus according to the theory described in the previous sections requires extensive numerical computations. We used a computer code called CASCADE, which was especially developed to calculate the evaporation residue mass and Z distributions. It starts from an excited compound nucleus with a spin distribution to be specified, calculates relative decay widths for neutron, proton, α-particle and γ-ray emission and generates matrices containing the population of the daughter nuclei as function of excitation energy and angular momentum. Then, by repeting this procedure, it follows automatically all possible decay sequences until the excitation energy has fallen below the particle threshold. Emission of deuterons can also be taken into account.

The size of the population matrices is 32 MeV in energy and $64\hbar$ in spin, when a 1 MeV energy step size is chosen and parity is neglected. If one choses 0.5 MeV steps and includes parity, which is usually only important in the last stages of the deexcitation process, then their dimensions are 32 MeV $\times$ $32\hbar$. The zero point of the energy and angular momentum scale is suitably chosen, so that the matrices always comprise the regions of interest.

At high excitation energy the complete deexcitation of a compound nucleus involves a large number of nuclei. In a typical case ($A_{\mathrm{CN}} \approx 40$, $E_{\mathrm{xCN}} = 70$ MeV) there are 30 nuclei with a transient population larger than 10 mb. The computation time depends very strongly on the excitation energy. At an IBM-370 computer a run takes 50 s for $E_{\mathrm{xCN}} = 40$ MeV and 500 s for 70 MeV (for 1 MeV steps, no parity). Because of the complexity of these calculations an efficient bookkeeping and a proper optimization concerning accuracy and computation speed are required. The accuracy is affected by the energy step length and by some cut-off parameters determining below

which level cross sections or decay probabilities can be neglected. General input data like nuclidic masses and transmission coefficients for the emitted particles are tabulated previously for the ranges of interest and stored permanently on disc.

3. Results

The theory described in the previous section was applied to the fusion reactions $^{19}F+^{12}C$, $^{16}O+^{27}Al$ and $^{19}F+^{27}Al$. The results are shown in comparison with the experimental evaporation residue mass distributions in figs. 3 and 4. It is very important that data taken at different beam energies are available. Whereas the energies far above the Coulomb barrier are most interesting as far as information about angular momentum effects are concerned, it is useful to have also data at lower energies, because there are essentially no free parameters in the calculation to which the results are sensitive. This is the reason why the time-of-flight data were supplemented by mass distributions obtained using γ-spectroscopic methods [7, 8]).

The structure of the experimental mass distributions is very well described by the calculations for all reactions and beam energies. In some cases, there is a slight

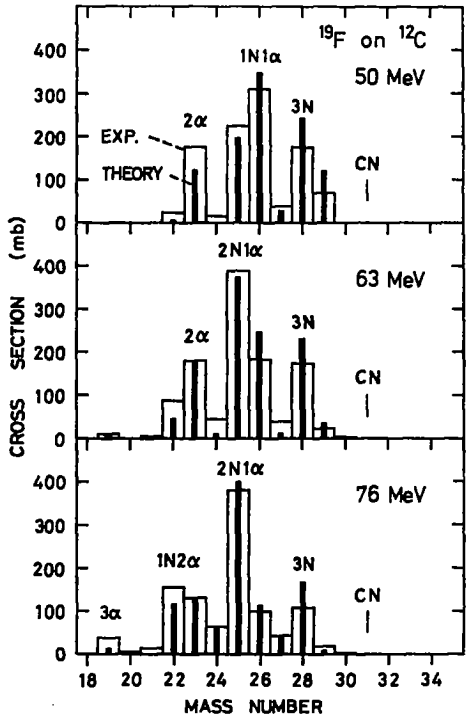

Fig. 3. Comparison between measured [2]) and calculated evaporation residue mass distributions in fusion reactions between ^{19}F and ^{12}C at different beam energies.

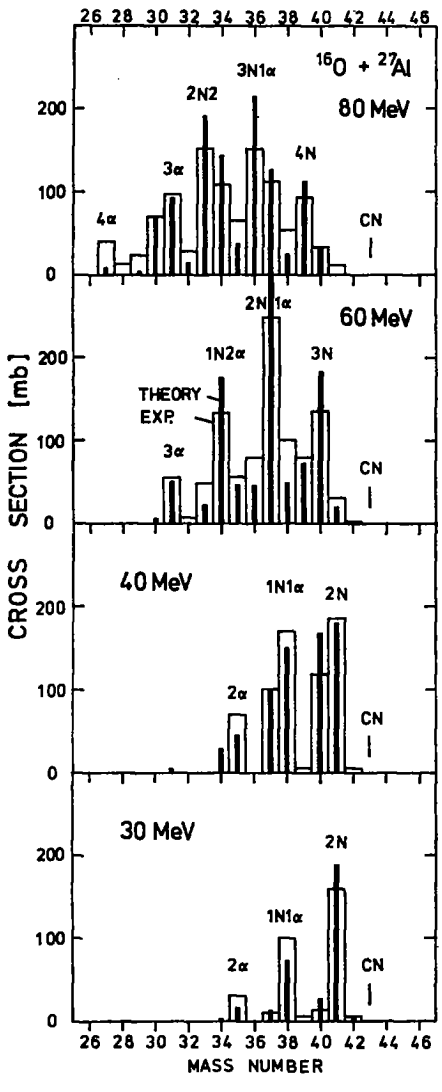

Fig. 4a.

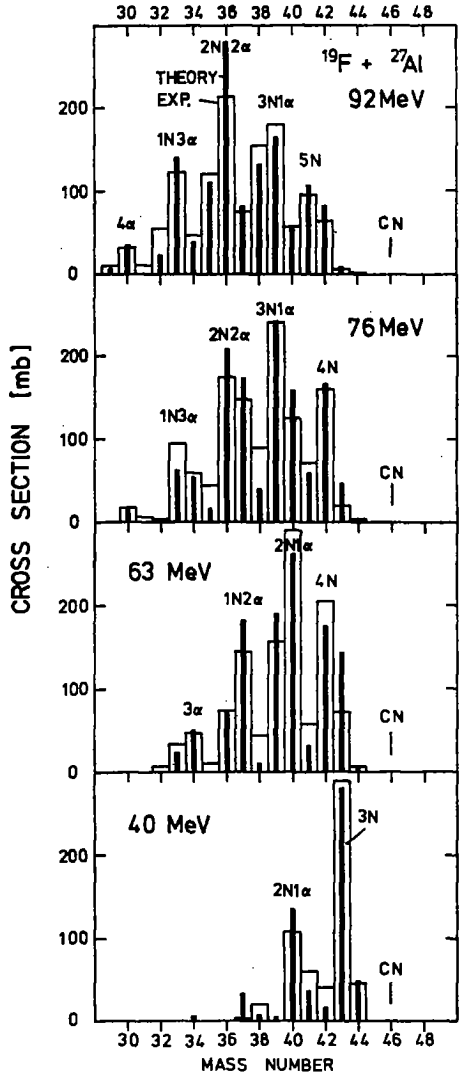

Fig. 4b.

Fig. 4. Experimental and calculated evaporation residue mass distributions in fusion reactions between ^{19}F and ^{16}O projectiles and a ^{27}Al target at different beam energies. Data are from Pfeffer *et al.* [6]), Dauk *et al.* [7]) (30 and 40 MeV ^{16}O on ^{27}Al) and Poletti *et al.* [8]) (40 MeV ^{19}F on ^{27}Al).

tendency to underestimate multiple α-emissions. At the lower beam energies this can only be due to inaccuracies of the transmission coefficients. This should become less important at higher beam energies, because the average emission energies also increase. Deviations often observed in the minima should not be taken too seriously. Firstly, the experimental data are subject to errors because of the finite mass resolu-

tion and, secondly, approximations in the calculation like the omission of deuteron emission or the cutoff of populations at the edges have the tendency to enhance the structure of the mass distributions and to cause errors in the calculated cross sections of extreme and unlikely decays.

In these calculations one has to specify a very large number of input parameters. Therefore, one has to make sure that as many as possible can be determined independently, at least to within certain limits, in order to obtain meaningful results. We proceeded as described in sect. 2 and tried to find a consistent set of parameters for all reactions and energies. The only exception is a higher reduced γ-width for the reactions on ^{27}Al. It should be noted that none of the parameters had to be varied seriously compared to what was expected before. These input data are discussed in the folowing paragraphs.

The spin distribution in the compound nucleus was determined from the experimental fusion cross sections. In the case of $^{16}O+^{27}Al$ a smooth interpolation between the data of Dauk *et al.* [7]), Pfeffer *et al.* [6]) and Kozub *et al.* [27]) was used. The parameters are given in table 2. The values for the diffuseness were chosen more or less arbitrarily, but the results are not sensitive to them. The transmission coefficients

TABLE 2

Excitation energies and angular momenta of the compound nuclei in the reactions studied

^{19}F on ^{12}C, CN = ^{31}P					
E_{lab}	(MeV)	50.0	63.2	76.0	
E_{xCN}	(MeV)	42.3	47.4	52.4	
σ_{CN}	(mb)	1040	1150	1070	
L_0	($\hbar$)	14.5	17.2	18.3	
d	($\hbar$)	0.71	0.95	1.10	
^{19}F on ^{27}Al CN = ^{46}Ti					
E_{lab}	(MeV)	40.0	63.2	76.0	92.0
E_{xCN}	(MeV)	48.9	62.5	70.1	79.4
σ_{CN}	(mb)	570 [a])	1150	1250	1250
L_0	($\hbar$)	14.5	26.5	30.4	33.5
d	($\hbar$)	1.0	1.0	1.0	1.0
^{16}O on ^{27}Al, CN = ^{43}Sc					
E_{lab}	(MeV)	30	40	60	80
E_{xCN}	(MeV)	33.1	39.4	51.9	64.6
σ_{CN}	(mb)	320	680	970	1050
L_0	($\hbar$)	8.8	15.5	23.2	28.0
d	($\hbar$)	1.3	1.3	1.3	1.3

The symbols are defined in sect. 2.

[a]) Extrapolated assuming $\sigma_{CN}/\sigma_R = 0.9$, σ_R from optical model calculations [6]).

for the evaporated particles were calculated from the optical model. The parameters used represent average parameters with a smooth dependence on the mass number. For neutrons we took the potentials given by Wilmore and Hodgson [28]), for protons those of Perey [29]) and for α-particles those of Huizenga and Igo [30]). The reduced γ-transition strengths as defined in subsect. 2.3 were roughly estimated from lifetimes of low-lying states in sd shell nuclei to be approximately $\xi_{E1} = \xi_{M1} = 0.5 \times 10^{-8}$, $\xi_{E2} = 0.3 \times 10^{-9}$ (or 0.001, 0.05 and 5 W.u. for E1, M1 and E2, respectively). These values are in very close agreement with the average transition strengths determined by Endt and Van der Leun [31]) for this region. They were used for $^{19}F+^{12}C$. For the reactions on ^{27}Al ten times larger values gave slightly better fits.

Concerning the determination of the level density parameters the procedure was as described in subsect. 2.4. Levels for region I were taken from the compilation of Endt and Van der Leun [32]) and supplemented by more recent data on high-spin levels where available. For region II the level density parameters a and Δ were determined individually for each nucleus. We started from the compilations of Vonach *et al.* [20]) and Dilg *et al.* [21]), which were supplemented by values determined by fitting the spectra of some sd shell nuclei. Using the fact that the effect of a variation of the parameter a can be compensated approximately by a proper change of Δ it was tried to systematize these values by defining a background, which varies smoothly from nucleus to nucleus, and by associating deviations as far as possible with shell closures or α-nuclei. This procedure makes it easier to interpolate and determine unknown values. The parameter r_0 was chosen to be 1.20 fm corresponding to an effective moment of inertia in region II of 85 % of the rigid-body value. This resulted in an yrast line which smoothly continues the known high-spin states. In the liquid-drop region, assumed to start at an excitation $U_{LDM} = 15$ MeV, the parameters were chosen according to the prescription given in subsect. 2.4 ($r_0 = 1.29$ fm, $\delta = 5 \times 10^{-4}$ and 2.5×10^{-4} for $^{19}F+^{12}C$ and $^{19}F/^{16}O+^{27}Al$ respectively).

4. Discussion

As shown in the previous section the experimental mass distributions can be described consistently using the theory of sect. 2. In this context one may ask how meaningful the fits are and what kind of information may be obtained from such analyses. One approach to answer these questions is to test the sensitivity of the results to parameter variations and to investigate the physical meaning of the parameters.

Fig. 5 shows what could be called theoretical error bars. The influence of taking another optical potential [by Satchler [33])] for calculating the α-particle transmission coefficients consists in an enhancement of nucleon compared to α-emission, which is not consistent with the data. Since this potential was more carefully deduced from elastic scattering of α-particles in this mass region than the one originally used one may interpret the result as an indication of the lowering of the Coulomb barrier due

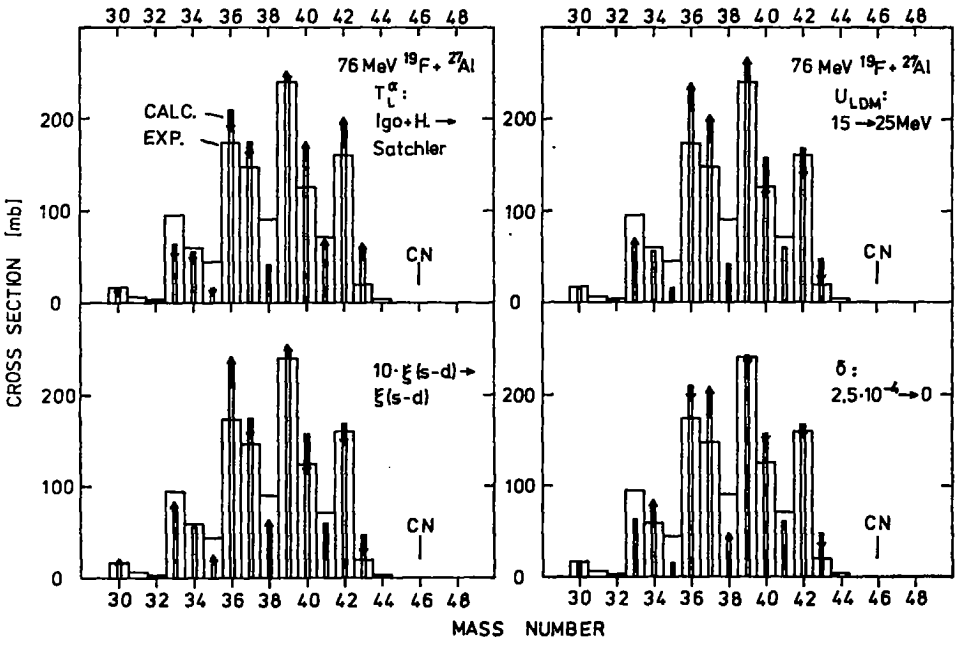

Fig. 5. Theoretical error bars. The influence of parameter variations on the calculated mass distribution is indicated by the length of the arrows.

to nuclear deformations at high angular momenta. A variation of the reduced γ-widths has a more complicated effect on the calculated mass distribution, although γ-decay competes only in the last decay step (see fig. 5). The level density parameters a and Δ in region II are rather well defined. The freedom which one has within the procedure given above has only little influence on the result. The same holds for a variation of r_0 in the range 1.20 ± 0.05 fm (in region II). It seems, however, that simple prescriptions for the level density parameters like $a = \frac{1}{8}A$ MeV^{-1}, $\Delta = 0.7, -0.7$ and -2.0 MeV for doubly even, odd-mass and doubly odd nuclei, respectively, generally lead to slightly worse fits, although this becomes apparent only if one looks more carefully at some details of the mass distributions.

The parametrization used here for the level densities seems to be rather complicated, and the question arises whether this is necessary. It is evident that the low-lying states are of great importance for the last decay step. Therefore they must always be included. Another assumption made here is that above a certain excitation energy the effects of the individual shell structure on the level density parameters a and Δ vanish. It would be very interesting if one could use these reactions for determining the transition energy. Unfortunately, it turns out that none of the reactions studied here is very sensitive in this respect. That means that even if one made the assumption that the empirical parameters a and Δ (of region II) were valid up to the compound nucleus excitation energy one would still obtain quite reasonable fits to the ex-

perimental mass distributions in most cases. This may seem very surprising at first. For example, in the reaction 80 MeV ^{16}O on ^{27}Al the nucleus populated by α-emission from the compound nucleus ^{43}Sc is ^{39}K, which has a relatively low level density compared to neighboring nuclei at excitation energies between 5 and 10 MeV. If it retained this property to high excitation energies, its calculated (transient) population would decrease to 35 % of that obtained with our standard model. However, ^{39}K cannot be observed because of further decays, and in the final products the effect is nearly entirely compensated. The missing decay chain CN-α3N, for example, is replaced by CN-3N1α and so on. The only exception is the cross section of $A = 31 =$ CN-3α, which must be produced via the first mentioned channel, and which decreases to 55 % of its original value. This example illustrates how complicated such studies can be. Apparently, the mass region $A = 20$–40 is not well suited for investigating how far shell effects in the level densities extent to high excitation. One would prefer heavier nuclei, where deviations from average values can be more clearly associated with shell closures. However, according to our model, the transition between regions II and III is also connected with a change in the moment of inertia and the shape of the yrast line. This is the main reason for the sensitivity of the results to the value of the transition energy (see fig. 5). The analysis of the present data and an earlier calculation for a heavier system [5]) indicate a rather low value ($U_{\mathrm{LDM}} = 15$ MeV).

It is particularly interesting to study the influence of the level density parameters a_{LDM}, $r_{0\mathrm{LDM}}$ and δ .They determine the relevant properties of the nuclei in the decay cascade in the so-called liquid drop regime (see subsect. 2.4). This region is expected to have the major influence on the gross features of the evaporation residue mass distribution and one may therefore hope to obtain new information about the behavior of highly excited nuclei from the analysis. The parameter a_{LDM} determines the slope of the level density as a function of excitation energy. A larger a_{LDM} puts more weight on smaller evaporation energies, and therefore also on nucleon emission. Values in the range $\frac{1}{9}A \leqq a_{\mathrm{LDM}} \leqq \frac{1}{7}A$ MeV^{-1} give similarly good fits, but very different values like $\frac{1}{11}A$ MeV^{-1} would be clearly inconsistent with the data. The radius parameter $r_{0\mathrm{LDM}}$ and the deformability δ determine the spin dependence of the level densities at high excitation. A change in $r_{0\mathrm{LDM}}$ can be essentially compensated by changing the deformability in the opposite direction, since both quantities determine the moment of inertia and the shape of the yrast line in a similar way in the restricted excitation energy range scanned by a reaction. Therefore, only one parameter needs to be varied. Keeping the value of $r_{0\mathrm{LDM}} = 1.29$ fm fixed one could try to determine the value of the deformability by fitting the cross sections of those residual nuclei which are most sensitive to it, with the constraint of course, that the rest of the mass distribution is correctly described.

As a result of the calculation for the reaction induced by 76 MeV ^{19}F on ^{27}Al fig. 6 shows the decomposition of the evaporation residue mass distribution into contributions originating from different angular momenta in the compound nucleus. Fig. 7 indicates the calculated dominant decay modes of a nucleus close to the compound

nucleus in this reaction as a function of excitation energy and angular momentum. Using this information and the one contained in fig. 6 one can construct the approximate and simplified "decay scheme" of the compound nucleus shown in the right-hand part of fig. 7. The result suggests that the different decay chains belong to different angular momenta ranges in the compound nucleus. Although this is true in the sense that it is certainly correct to say that pure nucleon decay is characteristic of small angular momenta and the decays with the highest α-multiplicities are characteristic of the highest compound nucleus spins, this statement must not be taken too literally. It should be noted that if the relative α-decay width is only 10 % per decay

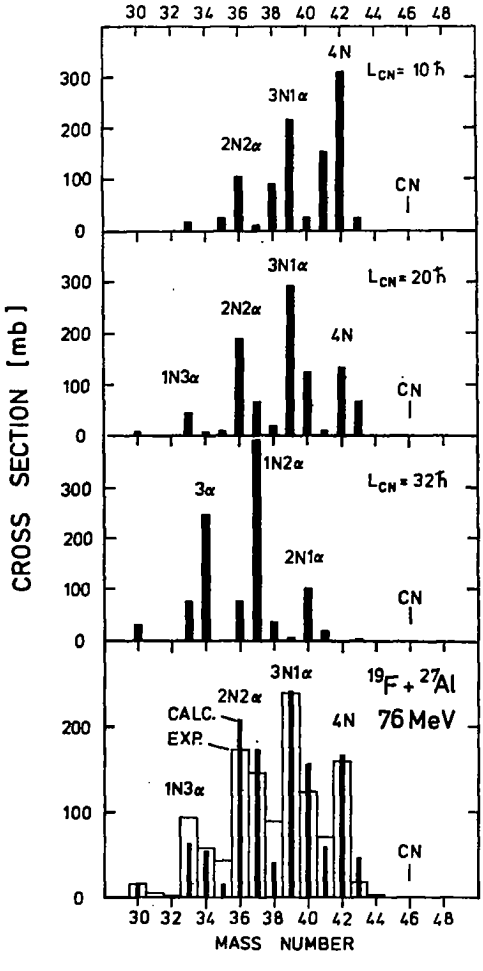

Fig. 6. Decomposition of the calculated evaporation residue mass distribution into contributions from different compound nucleus spins (normalized to 1000 mb). The sum of such distributions weighted by the partial formation cross sections gives the result shown at the bottom.

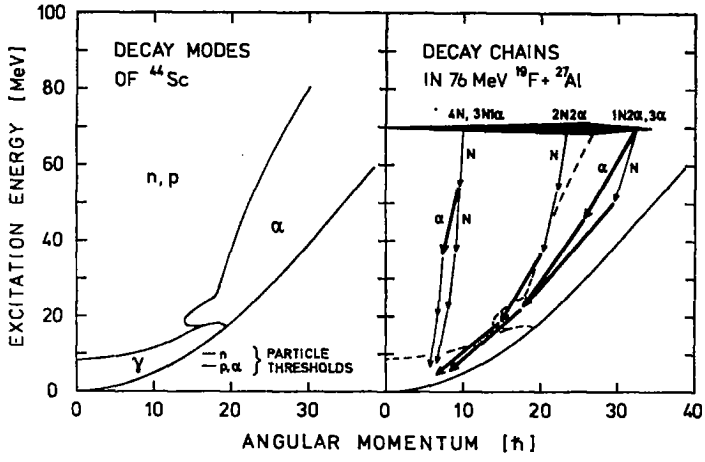

Fig. 7. Dominant decay modes (partial width > 50 %) for the nucleus ^{44}Sc. In the right-hand part of the figure, the most likely decay chains in the reaction 76 MeV ^{19}F+^{27}Al are indicated for different angular momenta of the compound nucleus ^{46}Ti. Heavy arrows for α-emission, thin ones for nucleons.

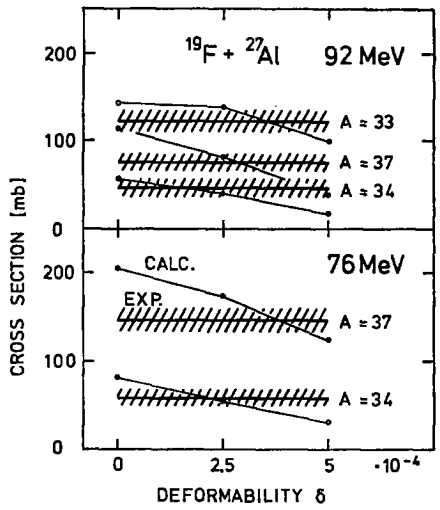

Fig. 8. Determination of the deformability δ by comparing the most sensitive calculated cross sections to the data. Compare with fig. 5. The hatching indicates the size of the experimental errors.

step–the approximate value for small spins–the probability for having a 3N1α decay in a four-step decay chain is already of the order of 30 %.

One recognizes from fig. 6 that the high-spin compound nuclei in the reaction 76 MeV ^{19}F on ^{27}Al decay essentially only into a few products, namely with mass A = 37(CN-1N2α) and A = 34(CN-3α). Consequently, the cross sections of these nuclei should be most sensitively influenced by the shape of the yrast line. A plot

(fig. 8) of the calculated yields for these mass numbers as a function of the deformability indicates that its value should lie in the range between $\delta = 2 \times 10^{-4}$ and 5×10^{-4} (see definition in subsect. 2.4). This is to be compared with the prediction of the theory of Cohen, Plasil and Swiatecki [24]) which corresponds to 2.5×10^{-4}.

5. Conclusion

In this work an attempt has been made to obtain quantitative information about nuclear properties which influence the decay of a highly excited compound nucleus by analyzing measured evaporation residue mass distributions. It was shown that the data can be described very well and with consistent sets of parameters for different systems and beam energies by applying the statistical theory for compound-nucleus reactions and taking into account emission of neutrons, protons, α-particles and γ-rays.

The success of the theory suggests that the various assumptions made may not be unreasonable. This conclusion, however, has to be made with some caution. Many assumptions, mainly those concerning the description of the level densities, represent approximations. One reason for using them is their simplicity and the fact that they introduce only a minimum of parameters necessary for describing expected phenomena. Some justification for this procedure lies in the fact that during the deexcitation process an averaging over a certain range in excitation and spin takes place. Therefore, the results are mainly sensitive to more global features, which can be described simply. In view of the large number of assumptions and parameters it is difficult to exclude the possibility that errors in the magnitude of parameters or in the functional dependence of a quantity like the level density mutually cancel. We tried to minimize this danger by simultaneously investigating a series of reactions at different energies. In this context, it is very important that the new experimental technique allows to measure all decay chains of the compound nucleus simultaneously.

The results obtained here may provide a basis for further applications. Typical for fusion reactions induced by heavy ions at beam energies well above the Coulomb barrier are the high excitation and the high angular momentum with which the compound nucleus is formed. Therefore, such analyses may yield information about the level densities of nuclei at high excitation, e.g. about the vanishing of shell effects. It would further be interesting to study the phenomena of shape variations of rotating nuclei as calculated by Cohen, Plasil and Swiatecki [24]) through their influence on the yrast line and the decay probabilities. It was shown in sect. 4 how one can proceed and how sensitive the mass distributions are. More data, in particular for heavier systems ($A_{CN} \approx 100$), would be desirable.

References

1) F. Pühlhofer, W. Pfeffer, B. Kohlmeyer and W. F. W. Schneider, Proc. Int. Conf. on nuclear physics, Munich, 1973, vol. 1, ed. J. de Boer and H. J. Mang (North-Holland, Amsterdam, 1973) p. 610

2) F. Pühlhofer, W. Pfeffer, B. Kohlmeyer and W. F. W. Schneider, Nucl. Phys. A244 (1975) 329
3) A. Weidinger, F. Busch, G. Gaul, W. Trautmann and W. Zipper, Nucl. Phys. A263 (1976) 511
4) J. D. Garrett, H. E. Wegner, T. M. Cormier, E. R. Cosman and A. J. Lazzarini, Phys. Rev. C12 (1975) 481
5) T. M. Cormier, E. R. Cosman, A. J. Lazzarini, H. E. Wegner, J. D. Garrett and F. Pühlhofer, Phys. Rev., to be published
6) W. Pfeffer and F. Pühlhofer, to be published
7) J. Dauk, K. P. Lieb and A. M. Kleinfeld, Nucl. Phys. A241 (1975) 170
8) A. R. Poletti, E. K. Warburton, J. W. Olness, J. J. Kolata and P. Gorodetzky, Phys. Rev. C13 (1976) 1180
9) R. G. Stokstad, Proc. Int. Conf. on reactions between complex nuclei, Nashville 1974, vol. 2, ed. R. L. Robinson, F. K. McGowan, J. B. Ball and J. H. Hamilton (North-Holland, Amsterdam 1974) p. 327
10) J. R. Grover and J. Gilat, Phys. Rev. 157 (1967) 802, 814 and 823
11) M. Blann, Phys. Rev. 157 (1967) 860
12) F. H. Ruddy, B. D. Pate and E. W. Vogt, Nucl. Phys. A127 (1969) 323
13) M. Uhl, Acta Phys. Austr. 31 (1970) 245
14) R. Stokstadt, D. Shapira, L. Chua, P. Parker, M. W. Sachs, R. Wieland and D. A. Bromley, Phys. Rev. Lett. 28 (1972) 1523
15) J. M. Blatt and V. F. Weisskopf, Theoretical nuclear physics (Wiley, New York, 1952)
16) T. D. Thomas, Nucl. Phys. 53 (1964) 577
17) W. Hauser and H. Feshbach, Phys. Rev. 87 (1952) 366
18) D. W. Lang, Nucl. Phys. 77 (1966) 545
19) J. Gilat, Phys. Rev. C1 (1970) 1432
20) H. Vonach and M. Hille, Nucl. Phys. A127 (1969) 289
21) W. Dilg, W. Schantl, H. Vonach and M. Uhl, Nucl. Phys. A217 (1973) 269
22) W. D. Myers and W. J. Swiatecki, Nucl. Phys. 81 (1966) 1; Ark. Fys. 36 (1967) 343
23) W. D. Myers, Nucl. Phys. A204 (1973) 465
24) S. Cohen, F. Plasil and W. J. Swiatecki, Ann. of Phys. 82 (1974) 557
25) V. S. Ramamurthy, S. S. Kapoor and S. K. Kataria, Phys. Rev. Lett. 25 (1970) 386
26) F. C. Williams, G. Chan and J. R. Huizenga, Nucl. Phys. A187 (1972) 225
27) R. L. Kozub, N. H. Lu, J. M. Miller, D. Logan, T. W. Debiak and L. Kowalski, Phys. Rev. C11 (1975) 1497
28) D. Wilmore and P. E. Hodgson, Nucl. Phys. 55 (1964) 673;
P. E. Hodgson, Ann. Rev. Nucl. Sci. 17 (1967) 1
29) F. G. Perey, Phys. Rev. 131 (1963) 745
30) J. R. Huizenga and G. Igo, Nucl. Phys. 29 (1961) 462
31) P. M. Endt and C. van der Leun, Nucl Phys. A235 (1974) 27
32) P. M. Endt and C. van der Leun, Nucl. Phys. A214 (1973) 1
33) G. R. Satchler, Nucl. Phys. 70 (1965) 177